Drought stress and hurricane defoliation influence mountain clouds and moisture recycling in a tropical forest

Martha A. Scholl[a,1], Maoya Bassiouni[b], and Angel J. Torres-Sánchez[c]

[a]US Geological Survey Water Resources, Reston, VA 20192; [b]Department of Crop Production Ecology, Swedish University of Agricultural Sciences, 750 07 Uppsala, Sweden; and [c]US Geological Survey Caribbean-Florida Water Science Center, Guaynabo, PR 00965

Edited by Robert E. Dickinson, University of California, Los Angeles, CA, and approved December 16, 2020 (received for review October 26, 2020)

Mountain ranges generate clouds, precipitation, and perennial streamflow for water supplies, but the role of forest cover in mountain hydrometeorology and cloud formation is not well understood. In the Luquillo Experimental Forest of Puerto Rico, mountains are immersed in clouds nightly, providing a steady precipitation source to support the tropical forest ecosystems and human uses. A severe drought in 2015 and the removal of forest canopy (defoliation) by Hurricane Maria in 2017 created natural experiments to examine interactions between the living forest and hydroclimatic processes. These unprecedented land-based observations over 4.5 y revealed that the orographic cloud system was highly responsive to local land-surface moisture and energy balances moderated by the forest. Cloud layer thickness and immersion frequency on the mountain slope correlated with antecedent rainfall, linking recycled terrestrial moisture to the formation of mountain clouds; and cloud-base altitude rose during drought stress and posthurricane defoliation. Changes in diurnal cycles of temperature and vapor-pressure deficit and an increase in sensible versus latent heat flux quantified local meteorological response to forest disturbances. Temperature and water vapor anomalies along the mountain slope persisted for at least 12 mo posthurricane, showing that understory recovery did not replace intact forest canopy function. In many similar settings around the world, prolonged drought, increasing temperatures, and deforestation could affect orographic cloud precipitation and the humans and ecosystems that depend on it.

ecohydrology | orographic precipitation | moisture recycling | disturbance hydrology | climate

The interaction between forests, atmosphere, and precipitation in mountainous areas is key to the maintenance of clean, steady water supplies, yet factors contributing to this outcome are still being identified. Forest-covered land impacts water and energy cycles at multiple scales (1). At a global scale, recent (2–4) and historical (5) evidence indicates that deforestation can affect precipitation patterns at great distances and over large regions (6). At a watershed scale, forest evapotranspiration returns large amounts of water to the atmosphere and regulates local meteorological conditions. Despite significant transpiration outflux, forest soils store and purify water for downstream uses, and forest land cover increases infiltration and moderates runoff to control flooding, thus often providing a net advantage for water resources (7–9).

Prevailing winds carry moist air from upwind oceans or landmasses; when this air is lifted by topography and cooled, orographic clouds form. Mountain regions are crucial to water supply worldwide (10) because orographic clouds produce precipitation, increase rainfall from regional scale weather systems (11), and, when in contact with mountain slopes (12), both add water and suppress evapotranspiration losses.

The lifting condensation level (LCL) is a quasi-planar feature in the atmosphere at the temperature and pressure that determine the transition of water from gas to liquid phase in rising air; its altitude can vary on timescales from diurnal to seasonal (LCL is just below cloud base; it can be "observed" on days with flat-bottomed clouds in the sky). Numerous studies hypothesized that global warming could raise the mean LCL or change frequency of coastal advective fog, thereby eliminating cloud-dependent ecosystems and hydrological inputs (13–17). Modeling studies in Central America (18, 19), the Amazon basin (20, 21), and the Western Ghats (22) suggested regional forest removal would decrease orographic precipitation due to lack of recycled evapotranspiration vapor input along air mass trajectories. In the Luquillo Experimental Forest (LEF), Scatena and Larsen (23) described higher cloud base, orographic rainfall decline, and temperature increase in the 3 mo after defoliation from Hurricane Hugo in 1989; however, insufficient data were available to confirm observations.

Few land-based measurements support modeled predictions of forest disturbance effects on mountain clouds (24, 25) because the complex interactions between these systems are difficult to detect from short-term data. Additionally, cloud base height cannot be measured by satellite at the spatial and temporal resolution required for hydrological analysis. This study presents in situ observations quantifying response of a mountain cloud system to forest disturbances (drought stress and canopy removal).

Study Design and Objectives

Mountain watersheds of the LEF (Fig. 1) in eastern Puerto Rico are strongly influenced by trade wind orographic uplift, causing rainfall and overnight cloud immersion (26–28) year-round. As

Significance

Mountains are focal areas for the transfer of water from atmosphere to land, but sustainable water provision under changing land cover and climate scenarios is not well understood. Our land-based measurements show mountain cloud formation in a coastal setting is significantly influenced by the condition of the windward forest, which regulates terrestrial energy and moisture cycles. We relate recycling of antecedent rainfall and diurnal patterns of temperature and water vapor along the mountain slope to mountain cloud occurrence. Cloud base height increased, and forest immersion frequency changed in response to both drought stress and hurricane defoliation. These findings inform resource management about how drought and deforestation may affect mountain precipitation, a major component of water availability worldwide.

Author contributions: M.A.S. designed research; M.A.S. and A.J.T.-S. performed research; and M.A.S. and M.B. analyzed data and wrote the paper.

The authors declare no competing interest.

This article is a PNAS Direct Submission.

[1]To whom correspondence may be addressed. Email: mascholl@usgs.gov.

This article contains supporting information online at https://www.pnas.org/lookup/suppl/doi:10.1073/pnas.2021646118/-/DCSupplemental.

Published February 9, 2021.

much as 5,000 mm mean annual precipitation (29) contributes to high soil moisture available for evapotranspiration, and canopy interception returns frequent light rainfall to the atmosphere. Forests in the study area are evergreen, and transpiration rates are high (30), driven by tropical temperatures and nearly constant trade winds. Isotopic tracers indicated that orographic precipitation (including cloud water) is a significant hydrologic input (31), crucial to sustaining streamflow during drought (32).

Monitoring in the LEF was designed to study effects of regional climate change on cloud base altitude and frequency of cloud immersion of the forested mountain slopes. In the marine-influenced climate of the LEF, we had an unprecedented opportunity to determine whether local orographic cloud formation is sensitive to land-based moisture recycled by the forest or is driven primarily by advected oceanic moisture interacting with topography. During the study, two extreme events (vegetation stress caused by drought and loss of vegetation caused by hurricane defoliation) provided observational evidence supporting the hypothesized links between the forest, local moisture and energy budgets, and the frequency and height (layer thickness) of orographic clouds.

From June 2015 to February 2016, a severe drought impacted the entire island (33). During drought, less canopy interception and increased vegetation stress from low soil water availability and high vapor pressure deficit (VPD) would be expected to reduce evapotranspiration and change surface-atmosphere feedbacks. On September 20, 2017, Hurricane Maria made landfall with 250 km · h^{-1} winds and as much as 963 mm of rainfall in 48 h over eastern Puerto Rico (34). Forest defoliation and damage (35, 36), tree mortality (37), landslides (38), and flooding (39) were widespread, along with catastrophic infrastructure damage. Defoliation would be expected to affect moisture and energy fluxes by reducing plant transpiration and canopy interception, changing evaporation from the land surface, and changing surface albedo, daytime shading, overnight radiative cooling, and wind buffering. The hurricane removed much of the forest canopy in the LEF, while the drought provided a period of vegetation stress without extreme canopy defoliation—these events created a natural experiment to examine interactions between the forest and hydroclimatic processes (*SI Appendix*, Fig. S1).

Our analysis of the coast-to-ridge area under prevailing wind flow (E to NE) includes air temperature (T) and relative humidity (RH, discussed herein as VPD) at five forest sites (617, 675, 794, 904, and 1,006 m); time-lapse imagery to detect forest cloud immersion at the 675- and 1,006-m sites; rainfall at 640- and 350-m sites; and ceilometer data at 10- and 100-m sites (when available), which covers undisturbed conditions, drought, and 14 mo posthurricane (April 2014 to November 2018). The analysis centers on the 675-m and 1,006-m sites, representing the forested mountain slope from median minimum cloud base altitude

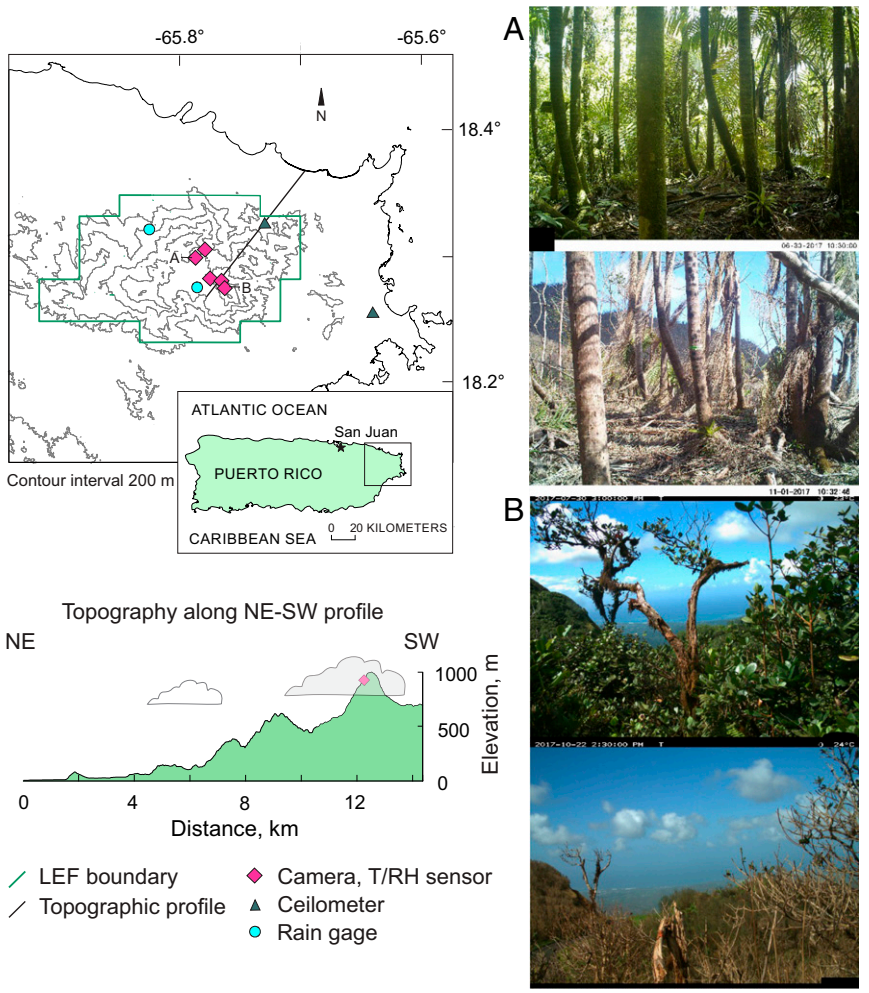

Fig. 1. The LEF in eastern Puerto Rico, showing location of measurements, topographic profile along the northeast slope of the Luquillo Mountains, and time-lapse camera images from the 675-m (*A*) and 1,006-m (*B*) sites before and after Hurricane Maria in September 2017. The image timestamps are local time (UTC-4).

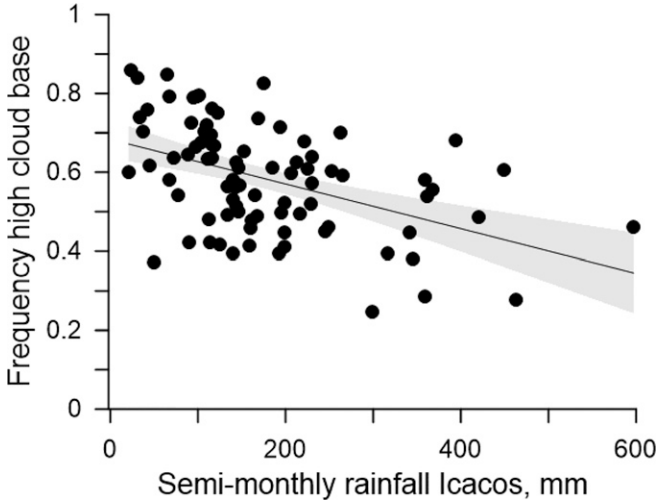

Fig. 2. The relationship between semimonthly rainfall and frequency of high-nighttime cloud base conditions on the windward mountain slope during study for the rain gauge at 642 m (Rio Icacos, USGS 50075000). The linear regression is $R^2 = 0.22$, $P = < 0.001$. The shaded area is 95% CI. The estimated-rainfall periods are not included.

(16) to the highest elevations on Puerto Rico (Fig. 1 and *SI Appendix*, Table S1).

The objectives of this study were as follows: 1) quantify feedback between local meteorological conditions and orographic cloud formation on the forested mountain slope and the anomalies that occurred with forest disturbance (drought and defoliation); and 2) determine whether forest disturbances caused cloud base to rise above mean observed altitudes, thereby decreasing thickness of the cloud layer and potentially reducing orographic precipitation inputs to the mountain forest.

Results

Clouds Generated on Mountain Slopes. Shallow cumulus clouds form over the upwind ocean (40) and move onto land in the trade wind flow; local clouds also form and persist on mountain slopes above the LCL from late afternoon through early morning (*SI Appendix*, Fig. S2). We compared in situ forest cloud immersion (27) with ceilometer-detected cloud base (41, 42) east and north of the mountains (Fig. 1). We assumed these represented ocean cumulus (at 10 m) and upwind coastal plain (at 100 m), respectively. During night hours (18:00 to 08:00), camera-observed cloud immersion frequency at 1,006 m averaged 7% and 24% higher than ceilometer-detected cloud base frequency ≤1,006 m at the 10-m and 100-m ceilometers, respectively. Nighttime mountain cloud formation varied seasonally; however, it did not match the seasonal pattern of ocean cumulus observed at the east coast. Rather, forest immersion frequency at 675 m coincided broadly with local wet and dry seasons (e.g., *SI Appendix*, Fig. S4) with a maximum from July to August and minimum from January to April. At 1,006 m, cloud immersion occurred on >75% of nights with little seasonal variation (*SI Appendix*, Fig. S2).

We quantified high cloud base altitude using simultaneous 30-min camera observations of 1,006 m cloud-immersed and 675 m clear. Because of extreme change in the daytime scene at the 675-m site after the hurricane (Fig. 1), we present results based on nighttime cloud immersion, which was highly consistent over time because it was determined by backscatter from cloud droplets in the camera's infrared flash [accompanying data set has 24-h record (43)]. Antecedent rainfall 48-h totals were positively correlated with cloud immersion frequency (*SI Appendix*, Fig. S5), with a higher correlation (0.4) for clouds observed at 675 m than at 1,006 m (0.2). Cloud base height was also negatively correlated with semimonthly rainfall amount at $P < 0.001$ (Fig. 2) for the rain gauge at Rio Icacos (642 m).

The frequency at which mountain slopes were immersed in clouds overnight was compared for undisturbed, drought, and 14-mo posthurricane periods. At 1,006 m, cloud immersion frequency during the drought was similar to undisturbed conditions but was higher than undisturbed conditions posthurricane (Fig. 3*A*). Immersion was much suppressed at 675 m during drought, while posthurricane immersion was lower for the first part of the night but increased toward sunrise (Fig. 3*B*).

Temporal and Spatial Anomalies in Local Meteorology during Disturbance. Departures from undisturbed mean annual and diurnal cycles of temperature and VPD (*SI Appendix*, Fig. S3) showed drought and defoliation anomalies were greatest at lower elevation during daytime hours. VPD anomalies at 675 m were >3× those at 1,006 m and featured notably drier daytime conditions through much of the posthurricane year. The defoliated system exhibited increased diurnal amplitude and warmer midday temperature at 675 m, while at 1,006 m, midday temperature was cooler and more variable overall, except the first 3 mo posthurricane were warmer at both sites during all hours. Drought changes were similar but lower in magnitude than those from defoliation.

Temperature gradients (T lapse rates) along the windward mountain slope were calculated from daily minimum (04:00) and maximum (13:00) values at the five sites (617 to 1,006 m). Night minimum lapse rates were similar during disturbed and undisturbed periods (mean = −4.6 °C · km^{-1}). Day maximum T lapse

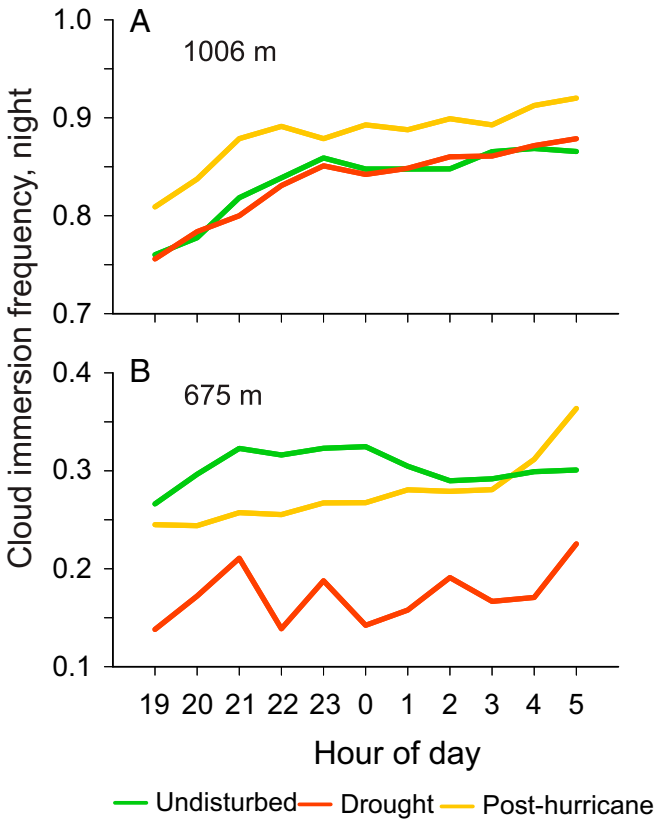

Fig. 3. The mean frequency of overnight cloud immersion during undisturbed, drought, and posthurricane (14-mo) periods at (*A*) 675 and (*B*) 1,006 m.

rates were steeper 0 to 4 and 5 to 14 mo after the defoliation (−9.6 and −8.8 °C · km^{-1}, respectively) compared to undisturbed and drought conditions (−5.7 and −6.6 °C · km^{-1}, respectively; Fig. 4*B*). VPD gradients were most often 0 at 04:00, reflecting 100% relative humidity along the mountain slope; at 13:00, gradients were steeper during drought and posthurricane periods (Fig. 5).

The evaporative fraction is the ratio of latent heat flux to total energy flux back to the atmosphere (latent plus sensible heat) estimated with a Bowen ratio approach. During undisturbed conditions, median evaporative fraction was 0.62, indicating that, overall in the LEF, latent heat flux from evapotranspiration was greater than sensible heat flux (Fig. 4*A*). The median evaporative fraction was 0.57 during the drought, 0.48 for 0 to 4 mo posthurricane, and 0.53 for 5 to 14 mo posthurricane (Fig. 4*A*), a range within that of a lower montane cloud forest in Mexico (44) where values ranged from 0.3 in the dry season to 0.7 in the wet season. During drought and after defoliation, transpiration was reduced due to an increase in stress from persistent high observed VPD (both disturbances) and decrease in leaf area index (defoliation). Lower evaporative fraction during forest disturbances quantified a shift in the surface energy balance to a greater fraction of sensible heat flux (Fig. 4*A*) and drove the observed spatiotemporal anomalies in temperature and VPD, which influence cloud formation.

Cloud Base Altitude with Drought Stress and Canopy Loss. The time series of high cloud base, temperature, and VPD gradients along the mountain slope, evaporative fraction, and antecedent rainfall anomaly (Fig. 5) shows cloud base position on the slope in response to moisture and temperature drivers. Clouds absent at 675 m and present at 1,006 m (high cloud base and thus thinner cloud layer; Fig. 4*D*) were observed frequently during drought, postdrought, and immediately posthurricane. During drought, high cloud base conditions began after ∼6 wk of below-normal rainfall; clouds returned to lower elevation during a "pause" in the drought in late summer, then rose again (Fig. 5). Cloud immersion data were unfortunately missing for drought fall/winter, when evaporative fraction recovered to undisturbed values despite below-normal rainfall; this may have been due to a decrease in vegetative stress from the middrought rain and fall temperatures.

Spring/summer preceding the hurricane (April 2017 to September 2017) had abundant rainfall and clouds present at both 1,006 and 675 m (low cloud base, thus thicker cloud layer) more than 50% of nights (Fig. 5). This pattern changed abruptly and significantly with defoliation from Hurricane Maria. Damage prevented observations until 4 wk posthurricane, but from 4 to 10 wk after the hurricane, overnight high cloud base predominated, accompanied by the steepest temperature and VPD gradients observed and, unlike the drought period, above-normal antecedent rainfall (Fig. 4 *C* and *D*). Cloud base height returned to average behavior in December 2017 (Fig. 5), though T lapse rates remained altered (Figs. 5 and 4*B*). Recovery of vegetation appeared in the increasing trend of evaporative fraction from ∼6 to 14 mo posthurricane (Fig. 5), supported by the time-lapse images (e.g., *SI Appendix*, Fig. S1).

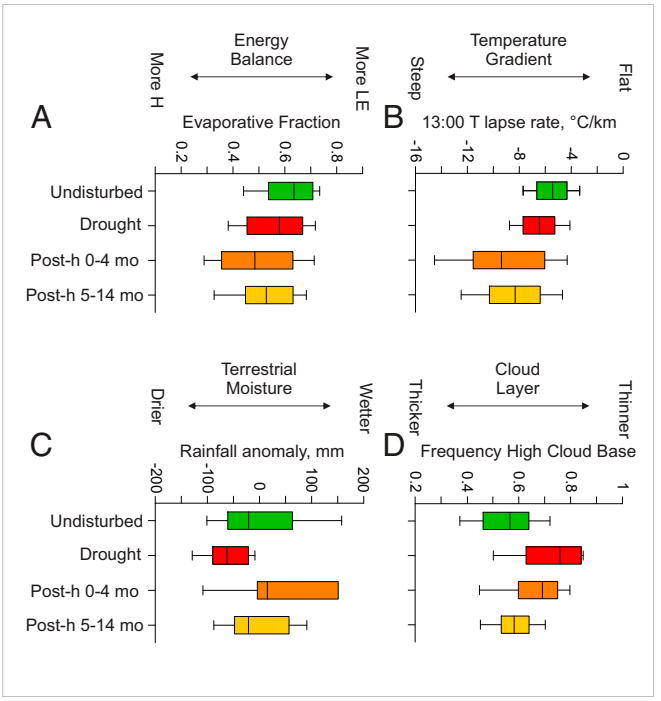

Fig. 4. The distributions of (*A*) evaporative fraction, (*B*) 13:00 T lapse rate, (*C*) rainfall anomaly (departure from long-term mean at the 642-m station), and (*D*) frequency of high cloud base for undisturbed, drought, 0 to 4 mo, and 5 to 14 mo posthurricane (post-h). H is sensible heat and LE is latent heat. The boxes represent interquartile range, and whiskers represent 10 and 90 percentiles. The plots used daily mean values of evaporative fraction and T and semimonthly mean values of high cloud base frequency and rainfall anomaly. The upper whisker on posthurricane rainfall bar is off-scale due to hurricane total.

Discussion

The two modes of disturbance allowed separation of terrestrial moisture versus vegetation effects on the orographic cloud system. With typical rainfall patterns but widespread loss of vegetation, the posthurricane energy balance was altered through effects on temperature buffering, canopy interception, and evapotranspiration, while during drought, plants closed their stomata to conserve water and avoid embolism, affecting transpiration but not canopy structure. Elucidating the role of forests in the orographic cloud system is critical to determine how land cover and climate changes may affect mountain slope water balances in similar geographic settings.

Antecedent Moisture, Canopy Structure, and the Cloud System. When precipitation over land is recycled to form mountain clouds, antecedent rainfall and locally generated clouds should be correlated. We found both cloud immersion frequency and cloud base height to be correlated to antecedent rainfall at 48-h (*SI Appendix*, Fig. S5) and semimonthly (Fig. 3) time scales. The response of the cloud system to sustained below-normal rainfall (2015 drought) was a shift to higher cloud base (thinner cloud layer on mountain slopes), while above-normal rainfall (summer 2017) was accompanied by low cloud base (thicker cloud layer). In general, high cloud base was correlated with low rainfall and steeper VPD gradient, but the immediate posthurricane period was different. Despite above-normal antecedent rainfall, both temperature and VPD gradients were steeper after defoliation, and high cloud base was more frequent (Figs. 5 and 4 *B–D* and *SI Appendix*, Fig. S2).

Before defoliation, the sensors at 675 m were below closed canopy with sparse understory, representative of the forest environment on the windward slopes above 600 m. The sensors at 1,006 m were at the top of the short cloud-forest canopy, representative of mountain ridge vegetation (Fig. 1 and *SI Appendix*, Fig. S1). Relatively consistent T lapse rates for the forested slope explain the frequent overnight cloud immersion in this setting (*SI Appendix*, Fig. S2), but the increase in cloud immersion at 1,006 m during the posthurricane period was unexpected (Fig. 3*A*). Our analysis indicates the loss of shading and the below-canopy microclimate buffer caused higher-amplitude diurnal temperature cycling and increased evaporative demand, so

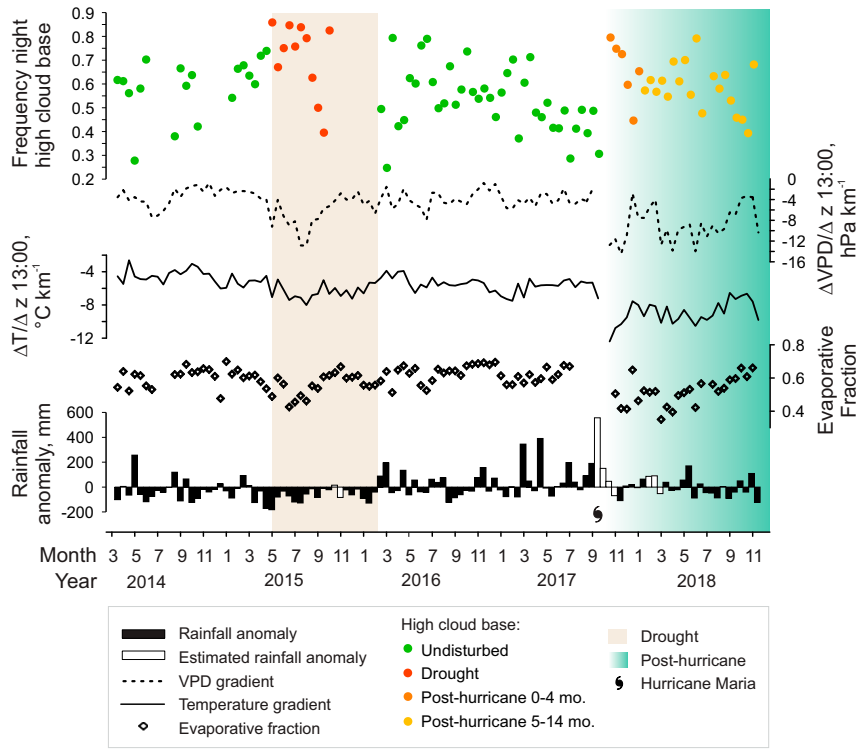

Fig. 5. The time series of the following semimonthly values: mean frequency of night (19:00 to 06:30) high cloud base conditions (675 m clear and 1,006 m immersed), mean 13:00 VPD and T gradients with elevation (z) from 610 to 1,006 m, mean evaporative fraction, and rainfall anomaly (departure from 27-y mean amount at Icacos, 640 m). The missing semimonthly rainfall data were filled with Daymet (white bars). There is no image data at 675 m from October 2015 to February 2016 (drought) and September 21 to October 15, 2017 (posthurricane).

the lower temperatures at 1,006 m condensed the increased moisture transported upslope that would have typically been retained under closed canopy.

The observed patterns represent different feedback from the diurnal temperature cycle and suggest daytime processes carried over to night cloud immersion. Posthurricane, the increased soil exposure, transpiration from proliferating understory plants and vines, and lack of subcanopy moisture trapping (e.g., ref. 45) all point to relatively more terrestrial-sourced moisture available to the atmosphere at night. With rainfall at normal levels, canopy loss led to temporary higher cloud base from higher temperatures, then persistent higher mountaintop cloud frequencies with an understory-prevalent, open-canopy forest structure.

Role of Evapotranspiration in Cloud Response to Disturbance. Satellite-based enhanced vegetation index (EVI) and normalized difference water index showed that the 2015 drought in the study area reduced productivity and leaf water content (46). Our results for the drought indicate limited moisture with increased daytime VPD at 675 m, but T lapse rates were similar to undisturbed conditions (Fig. 5). Overnight cloud frequency was much lower at 675 m while relatively unchanged at 1,006 m (Fig. 3). This caused a rise in cloud base but no decrease in mountaintop cloud frequency until well into the drought (*SI Appendix*, Fig. S2). These results are consistent with vegetation's water-use response to disturbance. During drought, latent heat flux is regulated by vegetation and the relative fraction of sensible heat flux increases.

The response of cloud base height to absence of transpiration was clear in the 6 wk after data collection resumed posthurricane. With canopy absent, daytime VPD and T lapse rates were above normal, evaporative fraction was below normal, and cloud frequency at 675 m dropped to <0.10, causing high cloud base despite above-normal antecedent moisture (Fig. 5 and *SI Appendix*, Fig. S2). Island-wide EVI composites (35) showed a major posthurricane decline then recovery of greenness by mid-November 2017, in agreement with other satellite indices (36, 47, 48). This recovery timing corresponds with the return of cloud immersion measured at 675 m, supporting our interpretation that understory transpiration reestablished conditions for lower cloud base levels. This vegetation recovery may have been greater on the coastal plain; in the study area, there was very little green, and forest canopy shading was still absent (*SI Appendix*, Fig. S1).

Decreased evaporative fraction during drought and defoliation points to the importance of vegetation in controlling heat flux and therefore the temperature influence on cloud base altitude during disturbance (higher sensible heat flux will cause higher LCL for a given specific humidity). The results strongly suggest that transpiration and vegetative cover are important factors in cloud base altitude, but questions remain about the necessary magnitude and timing of transpiration fluxes for sustainable cloud generation.

Implications for Forested Mountain Slopes as a Water Resource. Results given here agree with broad regional assessments (4, 18, 19, 49) and add evidence that local forest disturbance can have immediate and lasting effects on upslope cloud formation. The canopy defoliation, although temporary in this hurricane-adapted tropical forest (23), was a land-cover change similar to deforestation from logging, wildfire, or disease. This study provides evidence that forest cover on mountain slopes contributes to cloud generation and must be sustainably managed to mitigate negative effects of projected droughts and increased temperatures on water resources.

Back-trajectory analysis over the global tropics (21) showed a strong positive relationship between cumulative exposure of air masses to vegetation and the precipitation produced by those air masses. Other model-predicted effects of upwind regional deforestation on tropical montane cloud forests indicated an increase in cloud base altitude from increased sensible heat flux over land, but these regional models did not include direct measurements (4). We show conclusively that cloud base rose in response to hurricane defoliation, and temperature increased most at lower elevation, causing T lapse rates to steepen. Cloud immersion frequency decreased at lower elevation while increasing at higher elevation, suggesting moisture recycling along the slope shifted to a mode that was unregulated by vegetation, then evolved back as the forest recovered. Advected oceanic moisture interacting with topography likely results in a baseline level of mountain cloud immersion in this setting (*SI Appendix*, Fig. S2); this source may have contributed to relatively fast recovery from disturbance.

Rising cloud base was correlated with multidecadal climate shifts in the Hawaiian Islands, where steepening daytime T lapse rates corresponded to higher cloud base and marine boundary layer drying (24). The Hawaii observations are consistent with our results, although Puerto Rico's windward slopes are smaller in scale, and disturbance was the driving factor for cloud base rise. Similarly, radiosonde-derived decadal variations in mean-layer LCL for our study area (50) suggested that cloud base altitude is sensitive to regional or global patterns in climate. Canopy trimming experiments in the LEF at lower elevation (51) showed a timeframe of >2.8 y for canopy recovery, while in the Philippines and previous Puerto Rico hurricanes, damage-induced changes in streamflow returned to predisturbance conditions within a year (52, 53). Our time-lapse image data (*SI Appendix*, Fig. S1) indicated the former closed canopy had not been reestablished at 14 mo posthurricane.

The subtropics are projected to become drier over the 21st century, and minimum temperatures are increasing (54, 55). In this study, drought-driven rise in cloud altitude was mitigated by high-elevation temperatures cool enough for condensation, but our results indicate that compounded effects of drought with warmer minimum temperatures due to forest loss or regional warming present a significant risk for decrease in orographic precipitation. Mountain and coastal cloud systems occur in many settings (e.g., the Andean páramo, the California redwood forests, the Western Ghats, and northeastern Australia). For Puerto Rico, an increase in cloud base height of 200 m more than these observed disturbance effects would eliminate cloud-immersion precipitation on the mountain slopes, significantly affecting the water budget (31).

Summary and Conclusions

Both drought stress and hurricane defoliation caused changes in cloud layer thickness and frequency of cloud immersion in the Luquillo Mountains of Puerto Rico. These in situ observations of a coast-to-ridgetop system document how upslope clouds depend on recycling of downslope rainfall moderated by the condition of the forest. Antecedent rainfall, temperature, and VPD along the mountain slope were closely linked to cloud response. The severe 2015 drought in Puerto Rico, which induced water stress on the tropical forest, caused frequent periods of high cloud base, and decreased cloud immersion. Hurricane Maria in 2017 removed much of the forest canopy, after which cloud base rose briefly and cloud immersion frequency decreased at low elevation and increased at high elevation. Results were consistent with the removal of the forest's subcanopy microclimate layer, leading to increased amplitude of diurnal temperature cycling and increased land-surface moisture flux after defoliation. Though the understory rebounded quickly, the canopy recovered more slowly, and posthurricane changes in temperature and VPD were still present 14 mo after the event.

Mountain systems with persistent orographic clouds have not been well characterized, possibly because small-droplet precipitation that is not measured by standard rain gauges was assumed to be inconsequential. Nevertheless, cloud water deposition affects several components of the water budget, and its importance is becoming better understood. The tight coupling of the mountain cloud system to antecedent rainfall and disturbance patterns shown here clearly indicates that land-based moisture recycling drives orographic cloud formation in these mountains, with temperature lapse rate and forest cover (structure and transpiration) as important controls on cloud base height and immersion frequency. Better characterization of these systems would provide information to manage resources to mitigate adverse effects from climate and land use changes.

In mountain watersheds around the world, the interplay between steady prevailing winds, marine- and land-derived moisture, and mountains creates a natural precipitation recycling system that produces a water supply of great value. The results observed in this resilient, humid tropical system suggest that, in drier regions, both drought and deforestation could cause a loss of moisture recycling and its concomitant ecohydrological sustainability.

Methods

Site Description and Instrumentation. The LEF study area in eastern Puerto Rico (Fig. 1) has a tropical maritime climate, with undeveloped wet-tropical forest to cloud forest on north- to east-facing slopes dissected by steep-sided stream valleys. The Luquillo Mountains, at 18 °N, intercept the easterly trade-wind flow. The regional mean-layer LCL (approximate cloud base) is at 557 m, and the cloud-layer capping trade-wind inversion is found, on average, at 2,141 m (16). Our previous work rarely showed cloud immersion below the range of 675 m to 1,050 m, the maximum elevation. Diurnal and annual temperature cycles follow a typical Northern Hemisphere pattern, with low seasonal amplitude (~6 °C) due to latitude. Rainfall occurs year-round; winter is drier, and spring through fall have a bimodal wet season (*SI Appendix*, Fig. S4).

To monitor the cloud system, trail cameras (initially Bushnell Trophy Cam HD, later Reconyx PC900) and temperature/relative humidity (T/RH) sensors (Onset Computer Corp. U23-001 then -002) were placed from 617 to 1,006 m (Fig. 1). The study began March 14, 2014; images were collected until November 14, 2018, and T/RH data until June 5, 2019. The 675- and 1,006-m sites have the longest and most complete records and are used in all analyses except lapse rates, for which as many of five sites' data as available were used. Sensors were mounted in open air at ~1.5 m above the ground in open shade, then under shade panels when sensor model was changed after the first year. Standard error in T was ±0.21 °C and ±3.5% in RH (manufacturer's data); mean absolute T difference between sensor models was 0.3 and 0.2 °C for the 1,006- and 675-m sites, respectively, which was less than year-to-year variability. Readings were confirmed in the field at most visits with a digital psychrometer or wet-bulb/dry-bulb measurement. All T/RH sensors and most cameras were broken or lost either during Hurricane Irma (September 7, 2017) or Hurricane Maria (September 20, 2017) and were replaced in October and November 2017.

Time-Lapse Images and Cloud Immersion Frequency. Time-lapse images at 30-min intervals were processed to create a binary time series of cloud-immersed or clear conditions at 675 and 1,006 m; methods are given in ref. 27. Trail cameras were placed at ~2 m above the ground; this quantified in situ cloud immersion below the canopy at 675 m and at top of canopy at 1,006 m. Camera internal settings determined whether image was color or grayscale based on light conditions. Grayscale images were illuminated by infrared flash, causing backscatter when cloud droplets were present in the air. Images were separated into day (color, 09:00 to 16:30), twilight (color or grayscale depending on season and high overcast, 07:00 to 08:30 and 17:00 to 18:30), and night (grayscale, 19:00 to 06:30). An image-processing routine then classified images into clear and cloud-immersed categories using statistical methods (27). Dew point temperature (T_{dew}) and VPD were not a proxy for cloud immersion; relative humidity of 100% (VPD = 0 or $T \leq T_{dew}$) indicates that condensed droplets are possible but not necessarily present, as they may occur during rainfall or without affecting visibility. However, each

image classified by the algorithm as cloud-immersed also had to satisfy the condition of VPD = 0, which corrected 0.6% and 1.5% of the cloudy image classifications to clear at 1,006 and 675 m, respectively. Frequency of cloud immersion was calculated as immersed/total images for periods with at least 40% of data. Of 244 wk in the study, there were 38 and 15 wk omitted at 675 and 1,006 m, respectively.

Hourly nighttime cloud immersion frequency at 1,006 m and 675 m was determined for undisturbed, drought, 0 to 4 mo, and 5 to 14 mo post-hurricane periods (*SI Appendix*, Table ST1). At 1,006 m, both night and day images were comparable pre- and posthurricane because the camera was above cloud-forest vegetation and the reference scene was similar despite hurricane damage (Fig. 1 and *SI Appendix*, Fig. S1). At 675 m, though posthurricane daytime images are valid observations, the reference scene changed so significantly (Fig. 1) that only night cloud-backscatter observations were directly comparable between pre- and postdefoliation periods.

Cloud base altitude data from ceilometers at 10 m [Roosevelt Roads 2013 to 2019 (41)] and 100 m [US Forest Service Sabana Field Station 2013 to 2016 (42)] (Fig. 1) were used to compare frequency of upwind coastal-plain cloud base ≤ 1,006 m detections with frequency of camera-observed cloud immersion at 1,006 m. We used lowest reported level cloud base from Meteorological Terminal Air Report (METAR) format data from Roosevelt Roads and first quartile cloud base from Sabana. We assumed ceilometer observations represented the marine (10 m) and transitional marine-to-terrestrial (100 m) atmosphere, while image data on the mountain at 675 and 1,006 m represented clouds generated by topographic lift.

Temperature, Vapor Pressure Deficit, and Lapse Rate. Mean-field T and RH were recorded at 15-min intervals, and T_{dew} and VPD were calculated from the T/RH data (43). Temperature lapse rates and VPD gradients representing conditions along the windward slopes from 617 to 1,006 m were calculated from March 15, 2014 to June 5, 2019. Average T and VPD from the 4, 15-min values at 13:00 (maximum T) and 04:00 (minimum T) were used to calculate daily minimum and maximum elevation (z) gradients (dT/dz) in °C · km^{-1} (dVPD/dz in hPa · km^{-1}), by linear regression for all days having data from at least three elevations (after November 7, 2014) and regression R^2 value > 0.5.

Evaporative Fraction. Total energy transmitted back to the atmosphere is the sum of latent (LE) and sensible (H) heat fluxes. Evaporative fraction (EF) is the ratio of LE relative to total energy flux and was used to detect a change in the energy budget posthurricane and/or during drought that could be associated with vegetation status. Similar to the Bowen ratio (H/LE) (56), we assumed that, during daytime and clear conditions at both 675 m and 1,006 m, heat and water were transported with the same mixing rate (same turbulent diffusion coefficient). The evaporative fraction H/LE can thus be estimated as

$$EF = 1/(1 + \gamma(dT/dq)), \quad [1]$$

where γ is the psychrometric constant (0.0004 K^{-1}), dT and dq are differences between 1,006 and 675 m T, and specific humidity (q), respectively.

We calculated evaporative fraction using 30-min T and RH measurements, excluding values during nighttime and cloud-immersed conditions. We filtered evaporative fraction values out of range (0 to 1) and then averaged evaporative fraction by day.

Antecedent Rainfall. Rainfall at 642 m, ≤3 km southwest of the camera locations (US Geological Survey [USGS] 50075000 Rio Icacos rain gauge, Fig. 1; https://waterdata.usgs.gov/pr/nwis/uv?site_no=50075000) was used to determine 48-h antecedent moisture and semimonthly departure from long-term mean rainfall. With 27 y of data at 15-min resolution, the site represents the most complete rainfall record for higher elevation in the Luquillo Mountains. For missing semimonthly rainfall amounts in Fig. 5, the estimated rainfall amount was obtained from the linear regression of semimonthly rainfall (SRF) in millimeters from Rio Icacos site and Daymet (57) at the site coordinates for the study period:

$$SRF_{Icacos} = 1.16(SRF_{Daymet}) + 31.9, R^2 = 0.63. \quad [2]$$

Daily Daymet rainfall extrapolated from a 1-km^2 grid was not well enough correlated to daily site values to fill missing 48-h antecedent moisture values. Rainfall data at Icacos was unavailable posthurricane due to damaged equipment. We estimated the 48-h Hurricane Maria storm total rainfall at the site as 627 mm from Rio Icacos stream discharge and nearby rain gauge observations at USGS 50999958.

Long-term mean rainfall values (normals) at Icacos were calculated as the mean of all semimonthly periods from 1992 to 2018 with ≥12 d of data resulting in 3% omitted. To determine whether this mountain site was representative of windward-slope rainfall, semimonthly normals were calculated from El Verde field station (Fig. 1) at 350 m with 19 y of data and 14% omitted (https://luq.lter.network/data/luqmetadata127); seasonal patterns at the two elevations matched well (*SI Appendix*, Fig. S4).

Data Availability. Datasets used in the analyses were deposited in the ScienceBase repository, https://doi.org/10.5066/P9UQCN4T.

ACKNOWLEDGMENTS. Funding was provided from the USGS Climate Research and Development Program and the Luquillo Critical Zone Observatory, NSF 1331841. We thank A.E. Van Beusekom, US Department of Agriculture (USDA) Forest Service International Institute of Tropical Forestry (IITF) for insightful discussions. D.M. Hernández and the dedicated staff at USGS Caribbean-Florida Water Science Center in Guaynabo, Puerto Rico, provided technical and logistical support. We thank USDA IITF and El Yunque National Forest staff for coordinating site access; J.W. Harvey and J.B. Shanley for posthurricane field work; and G.A. Sexstone (USGS) and two anonymous reviewers for helpful comments. Any use of trade, firm, or product names is for descriptive purposes only and does not imply endorsement by the US Government.

1. D. V. Spracklen, J. C. A. Baker, L. Garcia-Carreras, J. H. Marsham, The effects of tropical vegetation on rainfall. *Annu. Rev. Environ. Resour.* **43**, 193–218 (2018).
2. D. Sheil, Forests, atmospheric water and an uncertain future: The new biology of the global water cycle. *For. Ecosyst.* **5**, 19 (2018).
3. D. V. Spracklen, L. Garcia-Carreras, The impact of Amazonian deforestation on Amazon basin rainfall. *Geophys. Res. Lett.* **42**, 9546–9552 (2015).
4. D. K. Ray, "Tropical montane cloud forests" in *Climate Vulnerability: Understanding and Addressing Threats to Essential Resources*, F. Hossain, R. A. Pielke, Eds. (Elsevier, 2016), 5, pp. 79–85.
5. G. B. Bonan, Forests, climate, and public policy: A 500-year interdisciplinary odyssey. *Annu. Rev. Ecol. Evol. Syst.* **47**, 97–121 (2016).
6. D. Ellison *et al*., Trees, forests and water: Cool insights for a hot world. *Glob. Environ. Change* **43**, 51–61 (2017).
7. L. A. Bruijnzeel, Hydrological functions of tropical forests: Not seeing the soil for the trees? *Agric. Ecosyst. Environ.* **104**, 185–228 (2004).
8. S. Filoso, M. O. Bezerra, K. C. B. Weiss, M. A. Palmer, Impacts of forest restoration on water yield: A systematic review. *PLoS One* **12**, e0183210 (2017).
9. U. Ilstedt *et al*., Intermediate tree cover can maximize groundwater recharge in the seasonally dry tropics. *Sci. Rep.* **6**, 21930 (2016).
10. D. Viviroli, H. H. Durr, B. Messerli, M. Meybeck, R. Weingartner, Mountains of the world, water towers for humanity: Typology, mapping, and global significance. *Water Resour. Res.* **43**, W07447 (2007).
11. A. M. Wilson, A. P. Barros, Landform controls on low level moisture convergence and the diurnal cycle of warm season orographic rainfall in the Southern Appalachians. *J. Hydrol. (Amst.)* **531**, 475–493 (2015).
12. L. A. Bruijnzeel, M. Mulligan, F. N. Scatena, Hydrometeorology of tropical montane cloud forests: Emerging patterns. *Hydrol. Processes* **25**, 465–498 (2011).
13. P. Foster, The potential negative impacts of global climate change on tropical montane cloud forests. *Earth Sci. Rev.* **55**, 73–106 (2001).
14. B. C. McLaughlin *et al*., Hydrologic refugia, plants, and climate change. *Glob. Change Biol.* **23**, 2941–2961 (2017).
15. B. Rastogi *et al*., Spatial and temporal patterns of Cloud cover and fog inundation in coastal California: Ecological implications. *Earth Interact.* **20**, 1–19 (2016).
16. A. E. Van Beusekom, G. Gonzalez, M. A. Scholl, Analyzing cloud base at local and regional scales to understand tropical montane cloud forest vulnerability to climate change. *Atmos. Chem. Phys.* **17**, 7245–7259 (2017).
17. K. C. Weathers, A. G. Ponette-Gonzalez, T. E. Dawson, Medium, vector, and connector: Fog and the maintenance of ecosystems. *Ecosystems (N. Y.)* **23**, 217–229 (2020).
18. D. K. Ray, U. S. Nair, R. O. Lawton, R. M. Welch, R. A. Pielke Sr, Impact of land use on Costa Rican tropical montane cloud forests: Sensitivity of orographic cloud formation to deforestation in the plains. *J. Geophys. Res. D Atmospheres* **111**, 960 – 975 (2006).
19. C. J. Still, P. N. Foster, S. H. Schneider, Simulating the effects of climate change on tropical montane cloud forests. *Nature* **389**, 608–610 (1999).
20. E. A. B. Eltahir, R. L. Bras, Precipitation recycling in the Amazon basin. *Q. J. R. Meteorol. Soc.* **120**, 861–880 (1994).
21. D. V. Spracklen, S. R. Arnold, C. M. Taylor, Observations of increased tropical rainfall preceded by air passage over forests. *Nature* **489**, 282–285 (2012).
22. D. K. Ray, V. S. Manoharan, R. M. Welch, Cloud cover conditions and stability of the Western Ghats montane wet forests. *J. Geophys. Res. D Atmospheres* **116**, D12104 (2011).
23. F. N. Scatena, M. C. Larsen, Physical aspects of hurricane hugo in Puerto Rico. *Biotropica* **23**, 317–323 (1991).
24. A. K. Kagawa-Viviani, T. W. Giambelluca, Spatial patterns and trends in surface air temperatures and implied changes in atmospheric moisture across the Hawaiian Islands, 1905-2017. *J. Geophys. Res. Atmospheres* **125**, e2019JD031571 (2020).

25. R. O. Lawton, U. S. Nair, R. A. S. Pielke Sr, R. M. Welch, Climatic impact of tropical lowland deforestation on nearby montane cloud forests. *Science* **294**, 584–587 (2001).
26. C. E. Asbury, W. H. McDowell, R. Trinidad-Pizarro, S. Berrios, Solute deposition from cloud water to the canopy of a Puerto Rican montane forest. *Atmos. Environ.* **28**, 1773–1780 (1994).
27. M. Bassiouni, M. A. Scholl, A. J. Torres-Sanchez, S. F. Murphy, A method for quantifying cloud immersion in a tropical mountain forest using time-lapse photography. *Agric. For. Meteorol.* **243**, 100–112 (2017).
28. F. Holwerda *et al*., Estimating fog deposition at a Puerto Rican elfin cloud forest site: Comparison of the water budget and eddy covariance methods. *Hydrol. Processes* **20**, 2669–2692 (2006).
29. S. F. Murphy, R. F. Stallard, M. A. Scholl, G. González, A. J. Torres-Sánchez, Reassessing rainfall in the Luquillo Mountains, Puerto Rico: Local and global ecohydrological implications. *PLoS One* **12**, e0180987 (2017).
30. W. Wu, C. A. S. Hall, F. N. Scatena, L. J. Quackenbush, Spatial modelling of evapotranspiration in the Luquillo experimental forest of Puerto Rico using remotely-sensed data. *J. Hydrol. (Amst.)* **328**, 733–752 (2006).
31. M. A. Scholl, S. F. Murphy, Precipitation isotopes link regional climate patterns to water supply in a tropical mountain forest, eastern Puerto Rico. *Water Resour. Res.* **50**, 4305–4322 (2014).
32. K. C. Clark *et al*., Tropical river suspended sediment and solute dynamics in storms during an extreme drought. *Water Resour. Res.* **53**, 3695–3712 (2017).
33. National Drought Mitigation Center, United States drought monitor. https://droughtmonitor.unl.edu/. Accessed 1 April 2019.
34. R. J. Pasch, A. B. Penny, R. Berg, Hurricane Maria (AL152017) 16-30 September 2017. National Hurricane Center Tropical Cyclone Report (2019). https://www.nhc.noaa.gov/data/tcr/AL152017_Maria.pdf. Accessed 1 September 2019.
35. J. Hall *et al*., Hurricane-induced rainfall is a stronger predictor of tropical forest damage in Puerto Rico than maximum wind speeds. *Sci. Rep.* **10**, 4318 (2020).
36. A. E. Van Beusekom, N. L. Alvarez-Berrios, W. A. Gould, M. Quinones, G. Gonzalez, Hurricane Maria in the U.S. Caribbean: Disturbance forces, variation of effects, and implications for future storms. *Remote Sens.* **10**, 1386 (2018).
37. M. Uriarte, J. Thompson, J. K. Zimmerman, Hurricane María tripled stem breaks and doubled tree mortality relative to other major storms. *Nat. Commun.* **10**, 1362 (2019).
38. E. K. Bessette-Kirton *et al*., Landslides triggered by hurricane Maria: Assessment of an extreme event in Puerto Rico. *GSA Today* **29**, 4–10 (2019).
39. M. J. Byrne Sr, "Monitoring storm tide, flooding, and precipitation from Hurricane Maria in Puerto Rico and the U.S. Virgin Islands, September 2017." *US Geological Survey Open-File Report* **2019** (2019). https://doi.org/10.3133/ofr20191065.
40. L. Nuijens, I. Serikov, L. Hirsch, K. Lonitz, B. Stevens, The distribution and variability of low-level cloud in the North Atlantic trades. *Q. J. R. Meteorol. Soc.* **140**, 2364–2374 (2014).
41. Noaa NCEI, Local Climatological Data, Roosevelt Roads station WBAN 11630. NOAA National Centers for Environmental Information. https://www.ncdc.noaa.gov/cdo-web/datasets/LCD/stations/WBAN:11630/detail. Accessed 1 February 2020.
42. G. González, *Luquillo Mountains meteorological and ceilometer data*. USDA Forest Service Research Data Archive (2017). https://doi.org/10.2737/RDS-2017-0023. Accessed 1 February 2020.
43. M. A. Scholl, A. J. Torres-Sanchez, S. F. Murphy, M. Bassiouni, Temperature, relative humidity and cloud immersion data for Luquillo Mountains, eastern Puerto Rico, 2014-2019 (2021). https://www.sciencebase.gov/catalog/item/5f7cc24f82ce1-d74e7db5531. Accessed 2 February 2021.
44. F. Holwerda, M. S. Alvarado-Barrientos, T. M. Gonzalez-Martinez, Surface energy exchange in a tropical montane cloud forest environment: Flux partitioning, and seasonal and land cover-related variations. *Agric. For. Meteorol.* **228-229**, 13–28 (2016).
45. F. Zellweger *et al*., Forest microclimate dynamics drive plant responses to warming. *Science* **368**, 772–775 (2020).
46. N. B. Schwartz, A. M. Budsock, M. Uriarte, Fragmentation, forest structure, and topography modulate impacts of drought in a tropical forest landscape. *Ecology* **100**, e02677 (2019).
47. T. Hu, R. B. Smith, The impact of hurricane Maria on the vegetation of Dominica and Puerto Rico using multispectral remote sensing. *Remote Sens.* **10**, 827 (2018).
48. P. W. Miller, A. Kumar, T. L. Mote, F. D. S. Moraes, D. R. Mishra, Persistent hydrological consequences of hurricane Maria in Puerto Rico. *Geophys. Res. Lett.* **46**, 1413–1422 (2019).
49. A. P. Williams *et al*., Urbanization causes increased cloud base height and decreased fog in coastal Southern California. *J. Geophys. Res.* **42**, 1527–1536 (2015).
50. P. W. Miller *et al*., A 42 year inference of cloud base height trends in the Luquillo Mountains of northeastern Puerto Rico. *Clim. Res.* **76**, 87–94 (2018).
51. A. E. Van Beusekom, G. González, S. Stankavich, J. K. Zimmerman, A. Ramírez, Understanding tropical forest abiotic response to hurricanes using experimental manipulations, field observations, and satellite data. *Biogeosciences* **17**, 3149–3163 (2020).
52. F. N. Scatena, E. O. Planos-Gutierrez, J. Schellekens, "Natural disturbances and the hydrology of humid tropical forests" in *Forests, Water and People in the Humid Tropics*, L. A. Bruijnzeel, M. Bonell, Eds. (Cambridge University Press, Cambridge, UK, 2005), pp. 489–512, 10.1017/CBO9780511535666.026.
53. J. Zhang, L. A. Bruijnzeel, R. Tripoli, H. J. I. van Meerveld, Water budget and run-off response of a tropical multispecies "reforest" and effects of typhoon disturbance. *Ecohydrology* **12**, e2055 (2018).
54. J. H. Bowden *et al*., High-resolution dynamically downscaled rainfall and temperature projections for ecological life zones within Puerto Rico and for the US Virgin Islands. Int. J. Climatol (2021). https://rmets.onlinelibrary.wiley.com/doi/epdf/10.1002/joc.6810. Accessed 28 January 2021.
55. J. Runkle *et al*., "Puerto Rico and the U.S. Virgin Islands" in NOAA State Climate Summaries, S.Champion et al., Eds. (NOAA, 2018). http://pubs.er.usgs.gov/publication/70197909. Accessed 28 January 2021.
56. W. Brutsaert, *Evaporation into the Atmosphere: Theory, History, and Applications* (Springer, Dordrecht, 1982), pp. 302, 10.1007/978-94-017-1497-6.
57. P. E. Thornton *et al*., Daymet: Daily Surface Weather Data on a 1-km Grid for North America; Version 3 (2016). https://dx.doi.org/10.3334/ORNLDAAC/1328. Accessed 26 February 2016.